Characterization of in-flame soot from balsa composite combustion during mass loss cone calorimeter tests

Gizem Okyay, Séverine Bellayer, Fabienne Samyn, Maude Jimenez, Serge Bourbigot

Accepted Manuscript

Characterization of in-flame soot from balsa composite combustion during mass loss cone calorimeter tests

G. Okyay, S. Bellayer, F. Samyn, M. Jimenez, S. Bourbigot

PII: S0141-3910(18)30205-2

DOI: 10.1016/j.polymdegradstab.2018.06.013

Reference: PDST 8578

To appear in: *Polymer Degradation and Stability*

Received Date: 2 November 2017

Revised Date: 30 March 2018

Accepted Date: 25 June 2018

Please cite this article as: Okyay G, Bellayer S, Samyn F, Jimenez M, Bourbigot S, Characterization of in-flame soot from balsa composite combustion during mass loss cone calorimeter tests, *Polymer Degradation and Stability* (2018), doi: 10.1016/j.polymdegradstab.2018.06.013.

Characterization of In-flame Soot From Balsa Composite Combustion During Mass Loss Cone Calorimeter Tests

G. Okyay, S. Bellayer, F. Samyn, M. Jimenez, S. Bourbigot*

[a] *Univ.Lille, CNRS, ENSCL, UMR 8207, UMET, Unité Matériaux et Transformations, F-59000 Lille, France*

Abstract

Soot is one of the degradation products of material burning, having the fingerprints of the conditions in which it is formed. In this work, in-flame soot was probed from flaming combustion of balsa core and its sandwich composite at different heat flux scenarios during mass loss cone calorimeter tests. Soot probing was performed by thermophoresis. Electron microscopy was performed to analyze the size of the particulate media at multiscale. The size of the aggregates and the primary particles were found to be inherent to scenarios, i.e. materials specifications and heat flux rates. Nanoscale structure of in-flame soot was consistent with the results of thermogravimetric analysis of emitted-deposited soot. This semi-quantitative study contributes to soot observations in fire scenarios and constitutes the first application of soot probing by thermophoresis in a bench-scale fire scenario simulated by cone calorimetry. Technique shall be used in future to support emitted soot and smoke data.

Keywords: soot, cone calorimeter, electron microscopy, multi-scale morphology, balsa composite

1. Introduction

For fire research and safety, the fire phenomenon and the response of materials exposed to it are examined through the properties of materials, their degradation pathways, physical and chemical properties, together with flame properties. In a fire scenario of polymer burning, the decomposition products in the gaseous phase include volatiles, condensables and particulate media (Brandrup et al. (1999)). An in-depth understanding of those products of combustion is essential both for experiments and simulations.

In general terms, soot represents carbon-rich material issued from the decomposed unburnt fuel molecules. In molecular stage, gaseous precursors are presumed to cluster until the nucleation of solid particulates and formation of aggregates, together with oxidation and surface growth reactions depending on the fuel and flame dynamics (Bockhorn (1994)). Soot is therefore one of the particulate degradation materials from combustion indicating the degree of incomplete burning in the gaseous phase. Its formation and morphology is directly dependent on the fuel type. In the gas phase of fire, soot clearly affects the thermal conditions because it is the major heat source and sink element. On the other hand, the nanoscale and mesoscale order of soot were reported to provide satisfactory information on the source identification in combustion systems (Vander Wal et al. (2010)). During a fire, the potential modifications in the mechanisms of soot formation are caused by the presence of additives, protective layers or by the external thermal constraints; the decomposition process of the materials and subsequent combustion dynamics are thus affected.

The exact soot formation pathways are still unknown for various types of fuels. So, the ex-situ observation of individual soot particles is a complementary tool to in-situ techniques in order to assess the flame dynamics, the fuel type and source identity (Michelsen (2017)). Soot probing by thermophoresis (Dobbins and Megaridis (1987)) is capable of providing single soot aggregates/agglomerates using microscopy observations. While this technique is widely used in combustion flames, its utilization is less common in fire

*Corresponding author: serge.bourbigot@ensc-lille.fr

domain. Some examples reported in literature are the flame soot analyzed from simulated and outdoor pool fires (Kearney and Pierce (2012); Shaddix et al. (2005); Jensen et al. (2005)). Very few studies reported multi-scale observations (Jensen et al. (2005)), and, so far, the in-flame soot from fires of polymeric materials has never been characterized at multiscale.

In bench-scale fire scenarios, soot emissions were reported for polymers and their fire retardant formulations in terms of the effect of fire retardancy on the emitted soot aerosols (Ngohang et al. (2015)), while some works reported the effect of additives (Naik et al. (2013); Rhodes et al. (2011)) and nanofillers (Motzkus et al. (2012)). Those studies were performed for soot in aerosol (i.e. emitted) form because most of the studies focused on the environmental deposition or the toxic effects of the particulates. Nonetheless, the probing of in-flame soot is an interesting alternative as it enables to probe the particulate media as close as possible to the production source. In earlier attempts on flame retarded (FR) etyhlene vinyl acetate and FR polyamide, fingerprints of flame retardancy were evidenced by their in-flame soot aggregates probed in cone calorimeter tests (Okyay et al. (2017)), and the primary particle size distributions complied with the combustion of the gaseous hydrocarbon decomposition products of polymers formerly reported (Girardin et al. (2015); Ngohang et al. (2014); Naik et al. (2013)). Technique enables single probing at specific instants instead of massive collection through filtering, preventing the restructuring of soot, hence providing more reliable data to comment on dynamics. In-flame probing is thereby a complementary approach to emitted soot and gases, enabling to trace the source, to comment on dynamics and on thermal conditions during testing. Note that soot particles are subject to modifications once they are outside the combustion process. This is especially true for the emitted type of soot because the particles can react with gases, or can adsorb them, once they are out of the flame and cooled down with exhaust gases. In that case, the particle collection through gaseous extraction is prone to errors if the denuding/filtration/dilution processes were not correctly set up while separating the gaseous media from particulate media (Ouf et al. (2010)). Direct probing is advantageous because high temperature treated soot does not undergo considerable morphology modification or surface reaction once outside the flame, if it has been stored properly in an isolated and moisture-free environment at ambient temperature, according to the reported protocols (Ouf et al. (2010)).

As a natural polymer, balsa material has a wide range of applications and research interests, such as sandwich composites used as structural components in marine applications (Morgan and Toubia (2014)). Balsa based flame retardant composites were also recently investigated (Kandare et al. (2014, 2016)). Compared to bare polymeric materials, composites with laminate skins exhibit more complex structural and thermal behaviors (Anjang et al. (2017)). Therefore, the main goal of this work aims at providing complementary data for further description of degradation materials from balsa, in order to trace the effects of thermal constraints and material intrinsic properties. To that end, balsa core and balsa sandwich composites were submitted to fire tests for soot probing and analyses. In this study, the particulate media were probed inside the flame during mass loss cone calorimeter tests, at 35 kW/m^2 and 50 kW/m^2 external heat flux rates mimicking mild and developed fires. For balsa composite testing, mass loss cone calorimeter tests were reported to provide good flammability data, even if they were reported not being completely representative of realistic fire conditions such as direct exposure to flame (Morgan and Toubia (2014)). Nevertheless in mass loss cone calorimeter tests, the external heat source is only radiative: evolved gases and soot products are completely inherent to degradation conditions and intrinsic to the material, contrary to hydrocarbon flame experiments where the material is subjected to an external flame. We will thereby examine the multiscale soot morphology to address the following questions: how are the flame soot particles affected when exposed to different external heat flux rates and to different constraints by addition of a skin layer (polyester resin filled in with glass fibers); how will the flame soot probing method of combustion be adjusted to bench-scale fire testing; how can the morphology of particulates be observed at multiscales.

2. Materials and methods

2.1. Virgin Material

Specimens tested in this study were obtained from commercial balsa composite: (1) a balsa core and (2) its composite form, having a core protected with skin layers made of glass fibers (non-woven) embedded in

polyester resin, with a core of 12 mm thickness and skins of 6 mm on both sides. All samples have a surface of 10x10 cm^2. In studies mimicking the real life application of balsa composites, the core layer thickness is much higher than in our study (Kandare et al. (2014)); in this work, observations were performed on a relatively thin balsa core to obtain a rapid burning of the material in mass loss cone calorimeter configuration for soot extraction, in order to minimize the time shift in probing times between the skin protected and the bare specimens.

2.2. Fire Testing

The reaction to fire testing of materials was performed on a mass loss cone calorimeter (MLCC) from Fire Testing Technology (FTT) according to standards ISO 13927 or ASTM E906. The samples were tested under the incident heat flux rates of 35 kW/m^2 and 50 kW/m^2 as depicted in Fig.1. At least two MLCC experiments were performed on each material in order to ensure repeatability within the error margins of $\pm 10\%$.

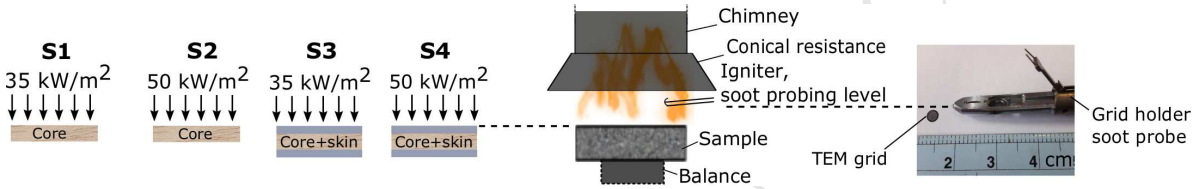

Figure 1: Illustration soot probing during scenarios 'S' in MLCC tests. The probing is performed on TEM grids, at mid-height of the gap between conical resistance and the sample surface.

2.3. Particle Sampling

Soot samples were probed inside the flame by impaction and thermophoresis on TEM (transmission electronic microscopy) grids (Dobbins and Megaridis (1987)), as illustrated in Fig.1. Lacey or holey carbon coated copper TEM grids were used. Probing was performed approximately ten seconds after the peak heat release rate (pHRR) on the output curve. The user indeed determines the probing instant during MLCC testing by actively monitoring the HRR curve. The time step of HRR data acquisition was 5 seconds. Therefore, the user can detect the pHRR at 'pHHR+5 seconds'. Then, user can perform probing at 'pHHR+10 seconds'. Probing instants of scenarios are illustrated in Fig.2.a.

2.4. Microscopy

Soot imaging was performed using Scanning Electron Microscopy in transmission mode (SEM/STEM) and Transmission Electron Microscopy (TEM). STEM images were taken using a JEOL 7800 FEG LV scanning electron microscope at 30 kV and 7 mA, using a retractable bright and dark field SEM STEM detector completed with Deben Gen5 electronics and a 12 position TEM grid holder. TEM and high-resolution (HRTEM) images were taken using a Tecnai G20 operating at 200kV. No special coating was applied on the soot specimens, as samples were not charged neither in STEM or TEM. Nonetheless, the observation times for HRTEM were kept as short as possible, due to damaging of soot graphitic layers at high beam exposure times at 200kV.

2.5. Image analysis

Image analyses were performed on electron microscopy recordings for a statistical distribution of primary particle size and the observation of multi-scale soot morphology. Primary particle and aggregate size measurements were performed by manual detection, as user dependent manual (completely manual or semi-automated) methods have been recently proven to show less uncertainties with ensured repeatability (Anderson et al. (2017)). All measurement, image processing and qualitative observations were performed using ImageJ and its plugins (Schneider et al. (2012)). The errors of mean primary particle size was estimated

from image treatments and resolutions: image smoothing needed to be performed on some SEM/STEM images (some image shifting was observed during recording) leading to errors in measurements. Note that no significant difference was reported when particles were observed with different sampling protocols. Only the primary particle diameter is susceptible to evolve when conserved in ambient air: however, the difference was reported to be limited to 1-3 nanometers for combustion soot due to storage artifacts (Ouf et al. (2010)). This value falls within the error range issued from image shifting and resolution which was estimated for particle measurements: mean diameter results are given accordingly.

2.6. Thermal Analysis

Thermo-gravimetric analyses (TGA) were performed on soot deposits obtained at 35 kW/m^2 and 50 kW/m^2, to verify a possible correlation between the in-flame soot structure and its thermal stability when emitted and deposited. Experiments were carried out on TA Instruments Discovery TGA, using $250\mu L$ open alumina pans covered inside with a gold foil, under an air flow of $20mL/min$. Experiments were performed twice for the repeatability check. Samples of 4.0 ± 0.2 mg were heated with an isothermal step at $40°C$ for 30 min followed by a heating ramp of $10°C/min$ up to $800°C$. Results were repeatable with a precision of $\pm 0.2\%$ residue mass for both samples.

3. Results and Discussions

3.1. Soot probing

In ideal conditions of gaseous combustion with enough oxidant, the final output of the chemical reactions is supposed to yield carbon dioxide and water with maximum heat release. However in realistic conditions and flame dynamics, the excess fuel or the lack of oxidant leads to incomplete combustion products such as carbon monoxide, hydrocarbon products such as PAH (polycyclic aromatic hydrocarbons) and soot (Bockhorn (1994)). In literature, studies on soot morphology consist of analyses at different scales: macro, micro and nano (Liati and Eggenschwiler (2010)) and in-flame soot probing is a common method to analyze soot morphology by ex-situ microscopy analyses for combustion flames. Accordingly, we will present multiscale semi-quantitative results on the probed particles, observed under electron microscope at different scales as depicted in Fig.2.b. Probing instants of scenarios are illustrated in Fig.2.a. The flame is in the highest fuel rich condition near pHRR (therefore highest reaction rates for the formation of flame soot) and the gases are at their highest thermal emissions. Therefore, this enables the intercomparison between different scenarios, in terms of thermal effects on soot at the most critical time step. The probing duration is around $\Delta t_p \leqslant 1s$ because this value is (i) small enough compared to HRR data acquisition steps (5 seconds), (ii) small enough to avoid perturbation on HRR curve (previously reported results with and without probing (Okyay et al. (2017))) and (iii) large enough compared to typical soot residence times of hundreds of milliseconds.

3.2. Macroscale/Microscale

At the macroscopic scale, the aggregation stage is important for the material-radiation interaction (Sacadura (2005)), and for the description of the emitted soot phase and their mobility (Sorensen (2011)), fragmentation and surface oxidation (Xu et al. (2003)); it can also give a qualitative idea on the volume fraction of soot. Here, the information is used to comment on dynamics, thermal effects and volume fractions. The size of the aggregates were computed over stacks of 20 to 30 images, over 80 aggregates for microscale measurements and over 200 particles for mesoscale measurements. Results are plotted on Fig.3 with example images corresponding to different scenarios. Results for both balsa core and sandwich, indicate slight decrease of the aggregate size with increasing heat flux. Two explanations are possible. First, the primary particles are slightly smaller (see the next paragraph 'Mesoscale') and second, as the macroscale gives information about agglomeration patterns, the number of particles contained in an aggregate is smaller at higher heat flux due to faster dynamics indicated by the higher peak heat release rate of 'S2' compared to 'S1, of 'S4' compared to 'S3' as depicted in Fig.2.a. On the other hand, we note the overall increase of the heat release rates due to addition of skin layer (Fig.2.a): this is directly reflected by highly agglomerated patterns of soot for 'S3' and 'S4' (Fig.3(e-h)) compared to tiny aggregates of 'S1' and 'S2' (Fig.3(b-d)). This will be

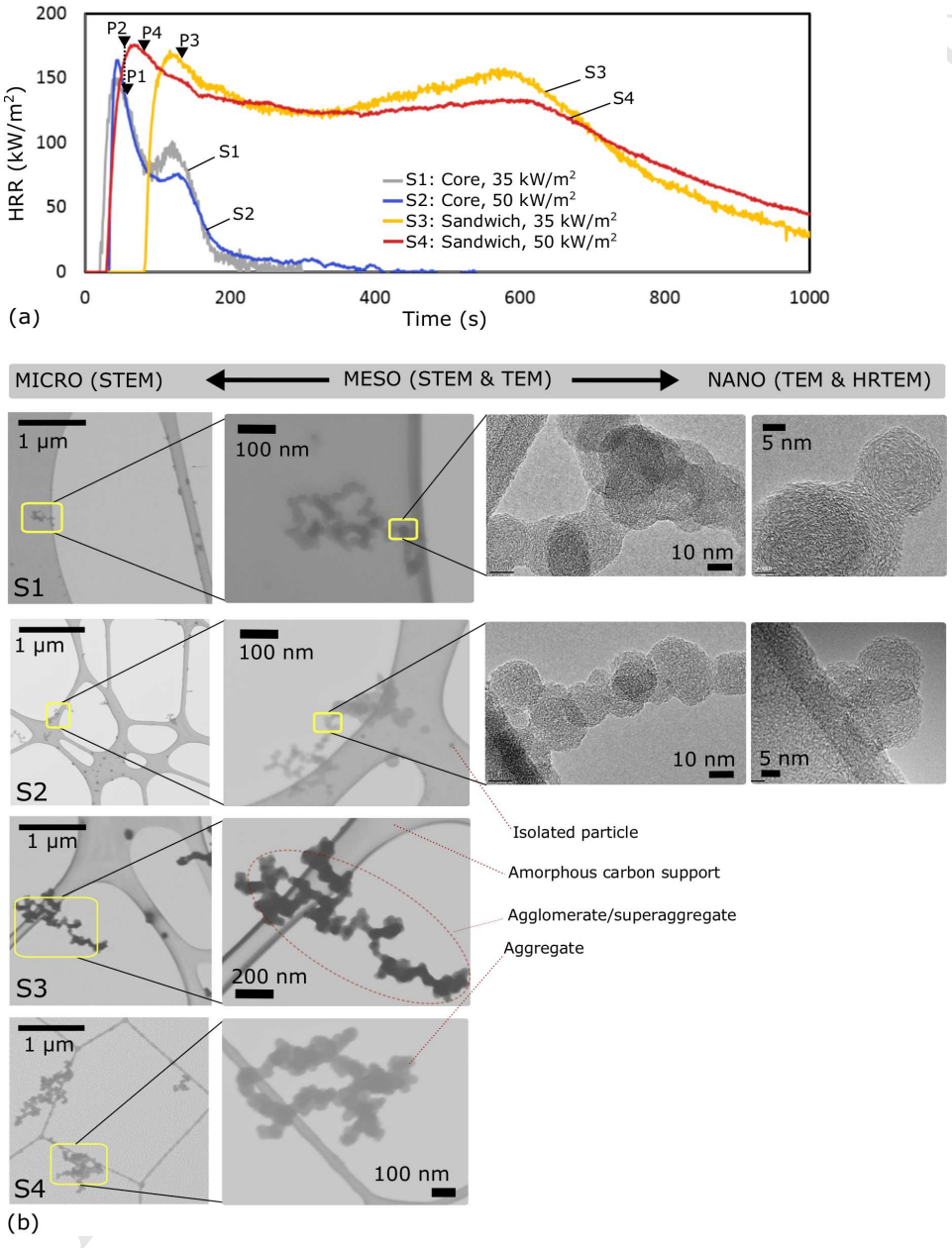

Figure 2: (a) HRR plots of scenarios 'S' with their corresponding soot probing instants 'P'. (b) Multiscale observations of morphology illustrated by the examples of microscopy recordings of soot at different scenarios.

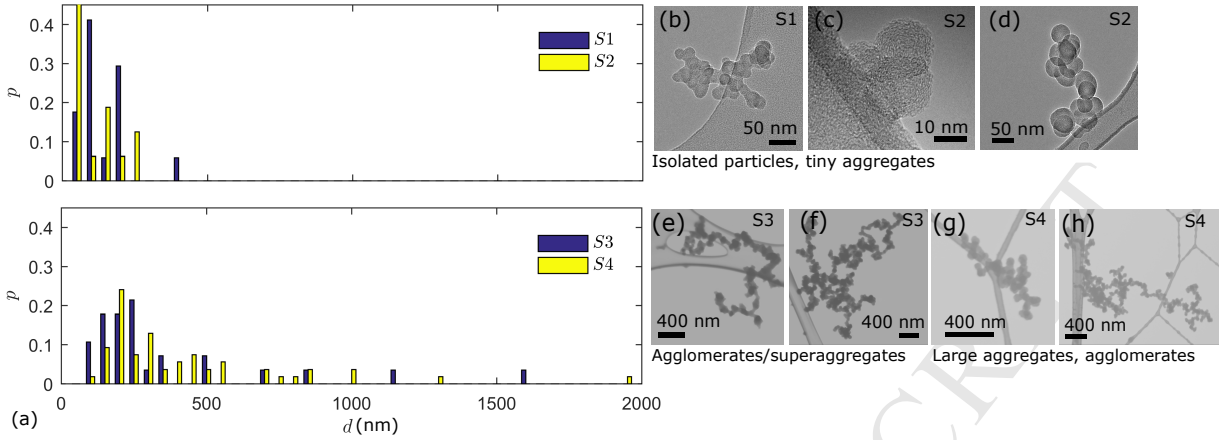

Figure 3: Results of the microscale image analyses, i.e. aggregate size. The probability is plotted versus the aggregate length d, determined according to mean chord length.

highlighted in section 3.6 on fire performance. In 'S3' and 'S4' the burning is fed both by the skin and the core layer where the lack of enough oxidant leaded to higher particulate concentrations. Therefore particles had more chance to collide, irreversibly stick and agglomerate for the latter configuration, as depicted in the microscale images of Fig.2.b.

Scenario	D_f (image)	D_p (image)	D_f (real)
S2	1,82 ± 0,10	1,30 ± 0,10	2,55 ± 0,10
S3	1,70 ± 0,10	1,48 ± 0,15	2,38 ± 0,10
S4	1,56 ± 0,10	1,55 ± 0,10	1,56 ± 0,10

(a)

(b)

Figure 4: (a) Example of fractal dimension D_f computations indicating the degree of compactness of aggregates. (b) Example of binarized images of aggregate for scenarios.

The size and the degree of compactness of soot shall define together the definition as an aggregate, agglomerate or superaggregate encountered in fire. In Fig.4, examples are presented for scenarios S2, S3 and S4. Quantitative definition of compactness is made by the mass fractal dimension D_f. The mass fractal dimension D_f and the perimeter fractal dimension D_p were determined by pixel counting on binarized images using reported procedures (Dhaubhadel et al. (2006)). The real mass fractal dimension was then determined by using semi-empirical correlations between D_f and D_p on 2D projection images (Jullien et al. (1994)). The dimensions were determined from the slope of the linear transition region of pixel counting plot; error terms were numerically estimated from the variation of the slope between maximum and minimum fractality limits, because the validity of D_f was found to be bounded by the mean particle size and mean aggregate length (Okyay (2016)). In soot and aerosol research, while aggregates (chemical bonding between all primary particles) have submicrometer dimension scale, larger aggregates were determined either as agglomerates (physical bonding between two aggregates) or as superaggregates (large dimension scales between $1-10\mu m$ and high compactness of around $D_f \approx 2.5$) (Dhaubhadel et al. (2006)). Therefore we can claim that some superaggregates were encountered in scenario 'S3' as depicted in Fig.3, according to results of Fig.4. If we compare the results between the balsa core with and without the skin layer, the size of aggregates is considerably increased by the addition of a skin layer, which considerably promotes the soot formation as shown in Fig.3.a. The reasons are again twofold: decomposition of the polyester resin promoted the soot formation, and the protection of the glass fibers inhibited the core combustion. This inhibition leaded to a more incomplete combustion (very large agglomerates) and changed the decomposition kinetics due

to thermal conditions of degradation (small particles combined with larger ones). This brings us to the determination of primary particle diameters.

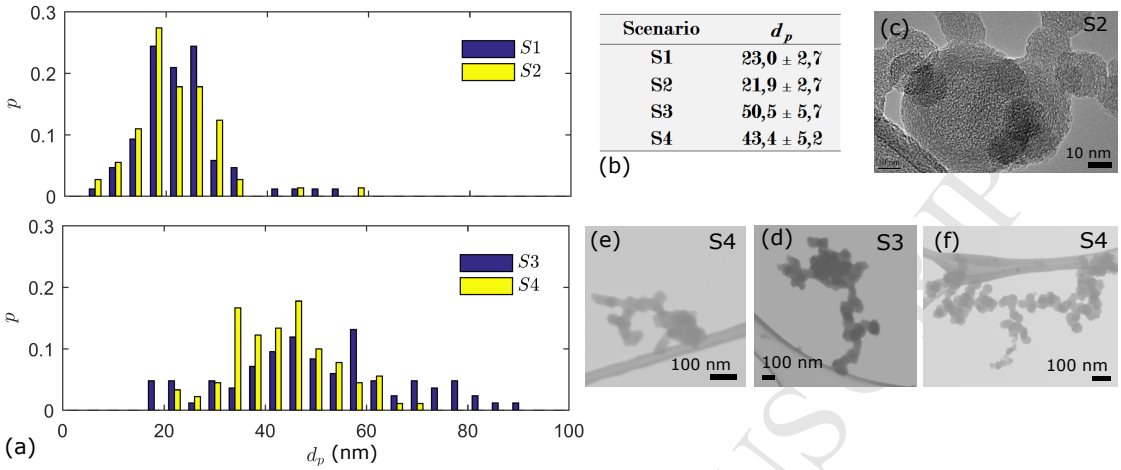

Figure 5: Results of the image analyses for soot primary particle diameter d_p. The probability is plotted versus the particle diameter determined by manual detection.

3.3. Mesoscale

The mesoscopic/microscopic investigation of the small aggregates and particles are important to interpret the combustion dynamics (Vander Wal (2015)). The analyzed particle diameters are plotted in Fig.5. The particle size distributions (Fig.5(a-b)) indicate that the mean particle diameter decreases slightly with increased heat flux scenario. On the other hand, the particle diameter is considerably increased by the addition of the skin layer as observed in Fig.5. The addition of a skin layer leaded to the production of superaggregate-like soot (Kearney and Pierce (2012)) as shown in Fig.5. Those aggregates reach few micrometers in maximum chord length, and their size distributions are multimodal as depicted in Fig.5.f. The balsa core produces individually recognizable primary particles as depicted in Fig.2.b corresponding to scenarios 'S1' and 'S2'. In scenarios 'S3' and 'S4', the organization is more compact; this is due to the polyester resin present in the skin layer: plastics were indeed reported to produce less recognizable and merged primary soot particles in some fire scenarios (Vander Wal et al. (2012)). Another interesting finding is the occasional observation of organic matter issued tar ball-like particles (Adachi and Buseck (2011)), as illustrated in the images of Fig.5. This can indicate some pyrolysis of organic matter in the balsa specimen and can be analyzed in future tests under inert atmosphere to detect sample purity.

At this scale, one important argument could be on the probing height above the sample surface. In this study, soot was always probed at the same height above the sample surface, which is not necessarily the same relative height for the flame at 35 and 50 kW/m^2 scenarios. This effect, important for combustion flames (Xu et al. (2003)), is neglected in our fire test. First reason is that the height difference between the flames were observed to be negligible during tests. Second, the flames in fire tests cover a specimen surface area of around 10x10 cm^2 and the soot probe sweeps those flickering flames trough a trajectory of few centimeters. Thereby the results are presumed to give averaged values over the specimen surface area.

3.4. Nanoscale

The investigation of soot at nanoscale is commonly used to retrieve information about its chemical and physical formation history (Vander Wal (2015); Botero et al. (2016)). It is closely correlated to the gas phase chemistry, including precursors, which are important for the determination of the flame structure and numerical combustion modeling (Frenklach (2002)). For balsa composite, complex correlations might occur between different chemistry (composition of skin layers) and different thermal constraints (external heat flux

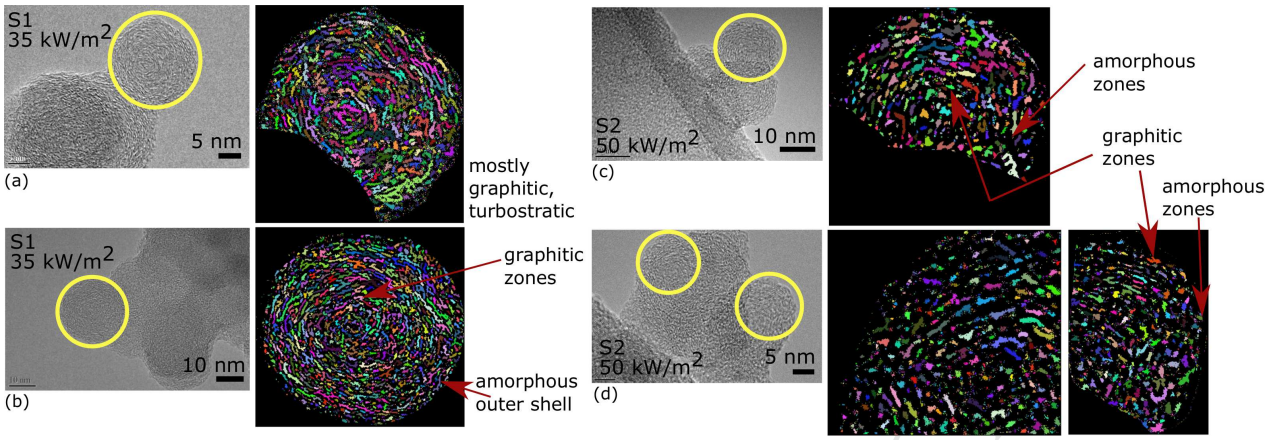

Figure 6: Examples of nanoscale images for soot extracted at different incident heat flux; image treatment performed to highlight the nanoscale order.

and addition of skin layers). As the skin layer promoted the formation of less recognizable primary particles, and as the nanoscale description of soot is directly related to chemistry, nanoscale analyses were performed on soot from balsa core burning in order to limit the problem to the thermal effects only.

Here, the study deals with the observation of the fringe organisation after image treatments (Botero et al. (2016)). Fig.6 shows examples of nanoscale images for soot extracted at different incident heat flux rates and the related image treatments performed to highlight the nanoscale order. Graphitic and amorphous organisation determine the reactivity of soot together with the curvature of molecules, related to the source and dynamics during soot formation. The graphitic organisation inside the particles changes their reactivity and oxidation properties (Vander Wal and Tomasek (2003); La Rocca et al. (2015)). As shown in Fig.6, the graphitic organisation of carbon declined with increasing external heat flux scenario; this was expected due to faster kinetics implied by the higher pHRR of 'S2' compared to 'S1' depicted in Fig.2.a. Moreover, there might be a small influence due to the differentiation between nascent and mature soot morphologies (Apicella et al. (2015)): the probe shall be more prone to catch nascent soot at faster kinetics at higher heat flux, and/or the particles do not have time to become mature and form turbostratic lattice fringes. The effect of probe height was presumed to be small at meso- and microscales, nonetheless the effect of probing height on the observation of nanoscale order can be more significant. Measurements shall be affected by probing at different heights above the sample, and also at variable probing times, because the residence time of the probe shall affect the thermophoretic forces and the perturbation degree of the flow fields around the sample holder.

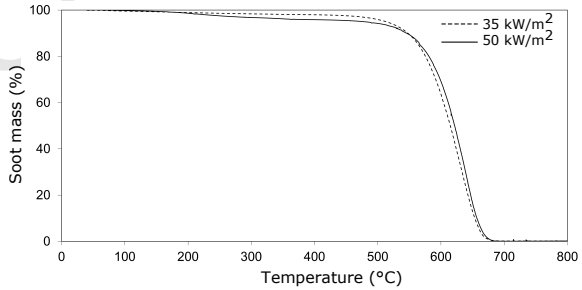

Figure 7: Thermogravimetric analysis in oxidant atmosphere for soot deposits collected on the MLC chimney.

3.5. Possible correlations of the reactivity with nanoscale observations

While soot is mainly composed of black carbon, it can contain some gaseous components and condensed matter attached or adsorbed on its surface (Bockhorn (1994)). During formation history of soot, external conditions, including thermal constraints, induce chemical and physical modifications in soot nanostructure and change the soot reactivity (Raj et al. (2014)). Therefore, in parallel to in-flame soot study, some TG analyses were performed on the emitted soot for possible correlations to nanostructure. (This step includes the overall internal and surface reactivity; this is not to be confused with the surface oxidation effects mentioned in microscale analyses above). To that end, few mg quantities of soot were collected in powder form by removing the MLCC chimney deposits after 35 kW/m^2 and 50 kW/m^2 scenarios. The deposition on the hot chimney walls would change the micro and mesoscale properties of soot once it is emitted, due to fragmentation. Although thermal treatments can modify the oxidation properties, it can reasonably be presumed that nanoscale properties remain constant up to thermal treatment temperatures of $400 - 500°C$ (Raj et al. (2014)). The chimney deposits were therefore considered to be representative enough of the flame soot for TGA.

The results of TGA under thermal oxidant environment are presented in Fig.7. Results indicated slightly higher content of volatiles and low weight species for soot of 50 kW/m^2 scenario, as shown in the range of $50 - 500°C$ in Fig.7. For example at $400°C$, the remaining mass was 98.0% for soot of 35 kW/m^2 and 95.8% for soot of 50 kW/m^2. This can be due to the higher amorphous structure of soot, as presented in the lower images of Fig.6. At higher TGA temperatures beyond $500°C$, soot of 50 kW/m^2 scenario have slightly lower reactivity. For example, at $600°C$, the remaining mass was 63.4% for soot of 35 kW/m^2 and 69.2% for soot of 50 kW/m^2. This can be explained by the nanostructure because the graphitic layers with lower curvature has lower tendency to undergo oxidation (Vander Wal and Tomasek (2003)). Visual observations indicate fringes with higher curvature for soot from lower heat flux scenario; as presented in Fig.6, soot of 35 kW/m^2 exhibits more like an onion shell structure. TGA results confirmed that soot of 50 kW/m^2 scenario was formed at a higher temperature. This latter conclusion might seem trivial, because we tested the same material compositions under different controlled heat exposures. Nevertheless, if different materials are to be correlated, nanoscale and thermal analyses can be an indication of the test temperatures and hot spots. In this latter case, the flammability and the stability of the different virgin materials can also be further investigated with their decomposition products.

3.6. Further implications for understanding the fire performance of composite

Results indicate that source/scenario identification is possible through particulate media when a limited combination of materials is studied (e.g. one synthetic and one natural material, same material in bare form or as the core of composite form, etc.). Comparing the core material and the composite, it was reported that the skin layer addition leads to high concentration of particulates. High compactness of superaggregates indicated not only high concentrations by skin layer addition, but also phenomena leading to a gelation-like cluster (Sorensen et al. (1998)) due to heavy sooting and/or restructuring of particles encountered in the aerosol phase of laminar diffusion flames (Sorensen et al. (2003)). On the other hand, this high concentration and compactnesses of particulates can potentially affect the heat emissions and thermal flux in the flaming combustion reactions. Even though the structural strength of a composite material depends on its fabrication combined with its intrinsic properties, the increase of the in-flame particulates due to skin layer addition could create potential hot spots in the gaseous phase, because the enhanced in-flame soot would increase luminous emission and heat release. This observation is similar to the augmentation of smoke by the formation of fire retardant char layer on balsa composite leading to enhanced pyrolysis of the core polymer (Kandare et al. (2014)). The rate of incomplete combustion is increased. This could, in return, speed up the structural failure of a composite at higher thermal exposures (Kandare et al. (2016)) due to the intrinsic decomposition properties of the burning material combined with the fabricated structure of sandwich panel, because the addition of skin layer promoted considerably the formation of soot. This can be verified in future studies by coupling the probing technique to in-situ particulate detections. Therefore for the design of polymeric composites and their fire retardant formulations, the reaction of material shall be carefully examined to find correct compromise between the structural strength, total heat and particulates

release. Thereby, our proposed probing technique can be a rapid and complementary approach to predict emission of particulates in flaming conditions.

4. Conclusion and Perspectives

In this work, the morphologies of in-flame soot of balsa core and of its sandwich exposed to MLCC test were characterized at multiscale. In summary, glass fiber skin promoted the soot aggregation and agglomeration, due to increase in incomplete combustion inhibiting fuel oxidation and due to decomposition of resin in the protective skin layer. Higher heat flux slightly decreased the aggregate and particle sizes, presumably due to faster flame dynamics. Soot was proved to be inherent to material physico-chemical/thermal properties in this fire test scenarios, according to aggregate and particle sizes. Higher heat flux reduced systematically the size of primary particles and the size of aggregates, regardless of the tested material. Addition of skin layers favoured systematically the polydispersity of the groups of aggregates in the same scenario, regardless of the heat flux scenario. Nanoscale structure reflected the combustion dynamics hence due to variable residence times of soot precursors at different energies. From a practical point of view, this study constitutes a first analysis for the in-flame soot of balsa composite in MLCC fire scenario. It reviewed the applicability of the source identification technique by soot probing, in order to examine and verify kinetics and thermal constraints together with the inherent properties of fire scenarios. It also contributes to the literature database on soot for numerous applications and proves the applicability of fundamental combustion results to fire research.

The technique shall be carefully applied against measurement errors which may arise from probing artifacts or from imaging artifacts. In this study, soot was probed in-flame, which is slightly different from the collection of soot particles in aerosol or emitted form in the exhaust gas or in the after flame zone. If there were any gases on/in the soot particles, it would be inherent in its formation inside burning gases and would not be an ex-situ artifact. Sublimated or evaporated agents would form drop-like shapes on the cold probe. Nevertheless, we did not observe, neither visually or by chemical analyses, any halogens, acids or other gas phase retardants condensed on our particles; any chemical elements other than carbon were not observed on soot surface. Once outside the flame, high temperature treated soot does not undergo morphology modification or surface reaction if it is stored properly in an isolated and humidity-free environment at ambient temperature, according to the reported protocols. A source of imaging error could be the pollution of the sample under the electron beam leading to a cracking of unburnt hydrocarbon molecules on soot surface. Or, the particle can undergo structural modification changing its compactness and nanoscale order. Those problems were avoided by working at low voltage of the electron beam for aggregate/particle measuring (in SEM/STEM), and by minimizing the imaging time at high magnification levels during nanoscale characterization (in TEM).

In prospective studies, the results shall be compared to the morphology parameters of exhaust soot and gas, for the study of mobility, oxidation and fragmentation. Comparisons shall be made for different fire scenarios and for possible correlations to physico-chemical properties of particulate and gaseous media. Similarly, for fire retardant mechanisms, such monitoring of the flame particulate media can confirm and elucidate the retardancy mechanisms in the gas phase.

Acknowledgement

This work has received funding from the European Research Council (ERC) under the European Union's H2020 - the Framework programme for Research and Innovation (2014-2020) / ERC Grant Advances Agreement n°670747 - ERC 2014 AdG/FireBar-Concept. It has benefited from the facilities of Centre Commun de Microscopie (SEM/STEM, TEM) of Lille. Johan Sarazin and Benjamin Dewailly are gratefully acknowledged for their technical assistance on MLCC specimen preparations.

Author Contributions

G.O. conceived the research; G.O. and S.Be. performed microscopy; G.O. performed the experiments, analyzed and compiled the data, developed functions as required for the analyses; G.O. wrote the article and prepared the figures; S.Bo., M.J., F.S. supervised the work; all authors contributed to the discussions during the studies.

References

Adachi, K., Buseck, P. R., 2011. Atmospheric tar balls from biomass burning in mexico. Journal of Geophysical Research: Atmospheres 116 (D5).

Anderson, P. M., Guo, H., Sunderland, P. B., 2017. Repeatability and reproducibility of tem soot primary particle size measurements and comparison of automated methods. Journal of Aerosol Science 114 (Supplement C), 317 – 326.

Anjang, A., Mouritz, A., Feih, S., 2017. Influence of fibre orientation on the tensile performance of sandwich composites in fire. Composites Part A: Applied Science and Manufacturing 100, 342 – 351.

Apicella, B., Pré, P., Alfè, M., Ciajolo, A., Gargiulo, V., Russo, C., Tregrossi, A., Deldique, D., Rouzaud, J., 2015. Soot nanostructure evolution in premixed flames by high resolution electron transmission microscopy HRTEM. Proceedings of the Combustion Institute 35 (2), 1895 – 1902.

Bockhorn, H., 1994. Soot formation in combustion : mechanisms and models. Springer-Verlag, Berlin.

Botero, M., Chen, D., González-Calera, S., Jefferson, D., Kraft, M., 2016. HRTEM evaluation of soot particles produced by the non-premixed combustion of liquid fuels. Carbon 96, 459 – 473.

Brandrup, J., Immergut, E., Grulke, E., 1999. Polymer handbook. 4th. Edn. New York: A Wiley-Interscience publication.

Dhaubhadel, R., Pierce, F., Chakrabarti, A., Sorensen, C., 2006. Hybrid superaggregate morphology as a result of aggregation in a cluster-dense aerosol. Physical Review E 73 (1), 011404.

Dobbins, R. A., Megaridis, C. M., 1987. Morphology of flame-generated soot as determined by thermophoretic sampling. Langmuir 3 (2), 254–259.

Frenklach, M., 2002. Reaction mechanism of soot formation in flames. Phys. Chem. Chem. Phys. 4, 2028–2037.

Girardin, B., Fontaine, G., Duquesne, S., Försth, M., Bourbigot, S., 2015. Characterization of thermo-physical properties of eva/ath: Application to gasification experiments and pyrolysis modeling. Materials 8 (11), 7837–7863.

Jensen, K., Suo-Anttila, J., Blevins, L., 2005. Characterization of soot properties in two-meter jp-8 pool fires. Sandia National Laboratories, Albuquerque.

Jullien, R., Thouy, R., Ehrburger-Dolle, F., 1994. Numerical investigation of two-dimensional projections of random fractal aggregates. Physical Review E 50 (5), 3878.

Kandare, E., Di Modica, P., Chevali, V. S., Gibson, G. A., 2016. Evaluating the heat resistance of thermal insulated sandwich composites subjected to a turbulent fire. Fire and Materials 40 (4), 586–598.

Kandare, E., Luangtriratana, P., Kandola, B., 2014. Fire reaction properties of flax/epoxy laminates and their balsa-core sandwich composites with or without fire protection. Composites Part B: Engineering 56, 602 – 610.

Kearney, S. P., Pierce, F., 2012. Evidence of soot superaggregates in a turbulent pool fire. Combustion and Flame 159 (10), 3191 – 3198.

La Rocca, A., Bonatesta, F., Fay, M., Campanella, F., 2015. Characterisation of soot in oil from a gasoline direct injection engine using transmission electron microscopy. Tribology International 86 (Supplement C), 77 – 84.

Liati, A., Eggenschwiler, P. D., 2010. Characterization of particulate matter deposited in diesel particulate filters: Visual and analytical approach in macro-, micro- and nano-scales. Combustion and Flame 157 (9), 1658 – 1670.

Michelsen, H., 2017. Probing soot formation, chemical and physical evolution, and oxidation: A review of in situ diagnostic techniques and needs. Proceedings of the Combustion Institute 36 (1), 717–735.

Morgan, A., Toubia, E., 2014. Cone calorimeter and room corner fire testing of balsa wood core/phenolic composite skin sandwich panels. Journal of Fire Sciences 32 (4), 328–345.

Motzkus, C., Chivas-Joly, C., Guillaume, E., Ducourtieux, S., Saragoza, L., Lesenechal, D., Macé, T., Lopez-Cuesta, J.-M., Longuet, C., 2012. Aerosols emitted by the combustion of polymers containing nanoparticles. Journal of nanoparticle research 14 (3), 687.

Naik, A., Fontaine, G., Samyn, F., Delva, X., Bourgeois, Y., Bourbigot, S., 2013. Melamine integrated metal phosphates as non-halogenated flame retardants: Synergism with aluminium phosphinate for flame retardancy in glass fiber reinforced polyamide 66. Polymer degradation and stability 98 (12), 2653–2662.

Ngohang, F., Fontaine, G., Gay, L., Bourbigot, S., 2014. Revisited investigation of fire behavior of ethylene vinyl acetate/aluminum trihydroxide using a combination of mass loss cone, fourier transform infrared spectroscopy and electrical low pressure impactor. Polymer Degradation and Stability 106, 26–35.

Ngohang, F.-E., Fontaine, G., Gay, L., Bourbigot, S., 2015. Smoke composition using mlc/ftir/elpi: Application to flame retarded ethylene vinyl acetate. Polymer Degradation and Stability 115, 89–109.

Okyay, G., 2016. Impact of the morphology of soot aggregates on their radiative properties and the subsequent radiative heat transfer through sooty gaseous mixtures. Ph.D. thesis, CentraleSupelec, Univ. Paris Saclay.

Okyay, G., Naik, A., Tranchard, P., Bellayer, S., Jimenez, M., Samyn, F., S., B., 2017. Physical characterization of carbonaceous products from fire and fire retardants: assessment of the impact on fire performance. In: Fire and Materials, FAM 2017. San Francisco, USA.

Ouf, F. X., Yon, J., Ausset, P., Coppalle, A., Maillé, M., 2010. Influence of sampling and storage protocol on fractal morphology of soot studied by transmission electron microscopy. Aerosol Science and Technology 44 (11), 1005–1017.

Raj, A., Tayouo, R., Cha, D., Li, L., Ismail, M. A., Chung, S. H., 2014. Thermal fragmentation and deactivation of combustion-generated soot particles. Combustion and Flame 161 (9), 2446–2457.

Rhodes, J., Smith, C., Stec, A. A., 2011. Characterisation of soot particulates from fire retarded and nanocomposite materials, and their toxicological impact. Polymer Degradation and Stability 96 (3), 277 – 284, fire Retardant Polymers Meeting Poznan 2009.

Sacadura, J.-F., 2005. Radiative heat transfer in fire safety science. Journal of Quantitative Spectroscopy and Radiative Transfer 93 (1), 5–24.

Schneider, C. A., Rasband, W. S., Eliceiri, K. W., Jul 2012. NIH image to imageJ: 25 years of image analysis. Nature Methods 9 (7), 671–675.

Shaddix, C. R., Palotás, Á. B., Megaridis, C. M., Choi, M. Y., Yang, N. Y., 2005. Soot graphitic order in laminar diffusion flames and a large-scale jp-8 pool fire. International Journal of Heat and Mass Transfer 48 (17), 3604–3614.

Sorensen, C., 2011. The mobility of fractal aggregates: a review. Aerosol Science and Technology 45 (7), 765–779.

Sorensen, C., Hageman, W., Rush, T., Huang, H., Oh, C., 1998. Aerogelation in a flame soot aerosol. Physical Review Letters 80 (8), 1782.

Sorensen, Christopher M and Kim, W., Fry, D., Shi, D., Chakrabarti, A., 2003. Observation of soot superaggregates with a fractal dimension of 2.6 in laminar acetylene/air diffusion flames. Langmuir 19 (18), 7560–7563.

Vander Wal, R., Pushkarev, V., Fujiyama-Novak, J., 2012. Fire signatures of spacecraft materials: Gases and particulates. Combustion and Flame 159 (2), 897–904.

Vander Wal, R., Tomasek, A., 2003. Soot oxidation: dependence upon initial nanostructure. Combustion and Flame 134, 1–9.

Vander Wal, R. L., 2015. Carbon nanostructure: Characterization by hrtem and xps and alteration by plh. in: CARBON 2015 spinoff workshop PyroMaN II, Dresden, Germany.

Vander Wal, R. L., Bryg, V. M., Hays, M. D., 2010. Fingerprinting soot (towards source identification): physical structure and chemical composition. Journal of Aerosol Science 41 (1), 108 – 117, special Issue for the 9th International Conference on Carbonaceous Particles in the Atmosphere.

Xu, F., El-Leathy, A., Kim, C., Faeth, G., 2003. Soot surface oxidation in hydrocarbon/air diffusion flames at atmospheric pressure. Combustion and flame 132 (1), 43–57.

- In-flame soot probed from balsa composite burning in fire tests
- Soot morphology studied at multiscale as a function of scenarios
- Composite skin layers promoted aggregation but reduced soot size
- Nanoscale structure confirmed TGA for reactivity and kinetics